

Different Topics Dealing With Sputtering of Cu, Ni and Cu-Ni Targets in Different Plasma Atmospheres

A. Rizk and H.N. Soliman

Physics Department, Faculty of Education, Ain Shams University, Roxy, Cairo, Egypt.

Abstract: The effects of ion bombardment on sputtering behaviour of Cu, Ni and Cu-Ni targets in inert and active gas atmospheres were investigated separately using a dc planar magnetron sputtering system. It was found that the hysteresis loops (current-voltage characteristics) obtained for the different sputtered targets were greatly affected by target material, gas type and gas pressure. The occurrence of these loops were due to: (1) residual ionization in case of using dry argon atmosphere; (2) formation of copper oxide and/or nickel oxide on the target surface when using oxygen in the glow discharge. The results also showed the formation of rough deposit circles on the outer face of each sputtered target and their diameters were depending on the above mentioned parameters. Scanning electron microscopy was also used to examine different morphological features formed on the sputtered targets in different plasma atmospheres.

Keywords: Cu; Ni; Cu-Ni; Magnetron Sputtering; Hysteresis Behaviour.

I. Introduction

Sputtering (i.e. the ejection of atoms from a surface due to ion bombardment) and accompanying processes are the basis of many ion-beam technologies such as ion-assisted deposition, ion-beam etching, surface polishing and cleaning, synthesis of repetitive surface nanostructures, and so on. Preferential (or selective) sputtering of one of the target components leads to the formation of an alternated layer which composition is different from the bulk.

Magnetron sputtering is a physical vapor deposition method which makes use of the ions created in a plasma to transfer materials from the target to a substrate.

A major difference between magnetron sputtering and other thin film deposition techniques such as thermal evaporation and chemical vapor deposition is that much higher energy can be input into the growing films with low substrate temperature. Thus, the deposition of high quality films with low substrate temperature is possible [1]. In addition to the low deposition temperature, magnetron sputtering has advantage on alloy and compound deposition by making use of a compound target or co-sputtering. Furthermore, the magnetron sputtering is a simple and low-cost technique for preparation of high-quality functional thin films of metals, alloys, nitrides, carbides or oxides due to the advantages of high deposition rates, excellent uniformity over large area substrates, and good controllability on the chemical composition and the physical properties of sputter deposited thin films [2-5]. Therefore, the magnetron sputtering technique has become established as the process of choice for the deposition of a wide range of industrially important coatings [6-9].

Recently, there has been a great interest in the study of ion sputtering of solid surfaces and numerous experimental and theoretical studies have been carried out to investigate the development of surface topographies [10-13].

Arising from these findings, it was considered useful to substantiate earlier studies and throw more light on different topics of sputtering Cu, Ni and Cu-Ni targets in inert and active gas atmospheres using a dc planar magnetron sputtering system.

II. Experimental Details

The Cu, Ni and Cu-Ni targets used in the present study were prepared from predetermined weights of spectroscopically pure copper and nickel metals. The ingot of each material was cold rolled at a 10% reduction per pass to a final thickness of 0.25 mm with intermediate steps of annealing during the rolling process. The elemental composition of the Cu-Ni alloy was obtained as Cu-10wt.%Ni by using energy-dispersive X-ray spectrometer as mentioned elsewhere [14]. Samples undergoing the previous steps were polished to obtain the as-received material.

Samples of each material ($1.5 \times 0.5 \times 0.025$ cm) were cut and electropolished using a suitable solution. To establish the right conditions for electro-polishing it was necessary to obtain the voltage-current relationship for the electrolyte and sample material used. An applied voltage of 3 V and corresponding current 0.2 A were found suitable for these samples and the electrolyte used at a temperature ranged from 288 to 293 K. The samples, after electropolishing were washed thoroughly with distilled H₂O and ethyl alcohol.

Scanning electron microscopy equipped with an energy-dispersive X-ray spectrometer (JEOL, JSM-5400, Radiation Research Centre, Cairo - Egypt) was used to examine the changes in surface morphology of different targets due to ion bombardment in different glow discharges.

On the other hand, sputtering experiments were performed using a dc magnetron sputtering system (Balzers SCD 040) which has been described in detail elsewhere [15]. Disc of 54 mm diameter and 0.25 mm thickness of each material was used separately as a target. Each target was electro-polished and cleaned in ethyl alcohol and distilled H₂O before sputtering experiments. The small cut samples were placed on outer surface of the cooled target. Therefore, the temperature of these samples was kept constant (at about 300 K) during sputtering process.

All sputtering experiments were carried out at constant input power of about 20 W in inert and active gas atmospheres at two chosen gas pressures of 0.05 mbar and 0.1 mbar. All samples were sputtered separately for 0.5 h. Then the sputtered samples were examined by scanning electron microscopy (SEM).

III. Results and Discussion

Hysteresis Behaviour:

The current–voltage characteristics for the different targets depend on several parameters such that target material, gas type and gas pressure.

Ion bombardment of Cu, Ni and Cu-Ni targets separately in a dry gas atmosphere of Ar⁺ (pressure of 0.05 mbar) resulted in the I-V characteristics shown in [Figure 1 \(a-c\)](#). It is interesting to note the formation of different hysteresis loops due to the lack of coincidence of the curves for increasing and decreasing voltage (time taken for each hysteresis loop is approximately 2 min). It can be seen from this figure that:

1) From the first insight, one can observe that greater current values are obtained from Cu target ([Figure 1a](#)) at all values of applied voltages as compared with those of both Ni and Cu-Ni targets as shown in [Figure 1\(b & c\)](#). This is referred to: (i) the high sputtering yield of Cu element as compared with that of Ni. The ratio of the sputtering yield of pure Cu with respect to Ni is $\frac{Y_{Cu}}{Y_{Ni}} \approx 1.53$ for 500 eV Ar⁺ bombardment [16] and (ii) the fact

that surface binding energy of Cu atoms is lower than that of Ni atoms [17, 18]. Consequently the probability of secondary electron emission is higher in case of sputtering Cu than that of Ni and this accordingly increases the current values.

2) As the applied voltage was increased, the corresponding current value increased for both Cu and Cu-Ni targets as shown in [Figure 1\(a & c\)](#). This increase in the current values was expected because the sputtering yield and thus the number of the emitted secondary electrons increases with increasing the applied voltage [19], and the total current is the algebraic sum of both gas ions and emitted secondary electrons.

3) For the Ni target ([Figure 1b](#)), as the applied voltage was increased, the corresponding current value decreased until a point is reached where further increase in the applied voltage was accompanied by an increase in the corresponding current value. The first part of this curve (from about 260 V to 360 V) is understandable if we recall the facts that: (i) Ni is a magnetic material and accordingly as the applied voltage was increased, most of the sputtered Ni atoms were attracted back again to the Ni target (which forms the outer face of the magnetron used) and (ii) occurrence of many collisions between returning Ni atoms and newly sputtering atoms. On the other hand, further increase in the applied voltage above 360 V (provides sufficient energy for the incident ions so the released sputtered atoms were able to overcome the back attractive magnetic force) was accompanied by an increase in the corresponding current value due to an increase in the sputtering yield and accordingly secondary electron emission.

4) For the Cu target ([Figure 1a](#)), as the applied voltage is decreased rapidly, the corresponding current values depart to higher values from those previously obtained in the first path of the cycle due to the slow deionization process of the gas. It is believed that the hysteresis loop obtained in this case is caused by the presence of residual ionization coming from the first path of the cycle beside those formed at each applied voltage. On the other hand, for both Ni and Cu-Ni targets as shown in [Figure 1\(b & c\)](#), as the applied voltage is decreased rapidly, the corresponding current values depart to lower values from those previously obtained during the first path of each cycle. It is believed that the lower current values obtained in these two cases were due to the redeposition of some sputtered Ni atoms (due to their attractive magnetic force to the target) on the target surface causing a decrease in the total number of sputtered atoms and emitted electrons leading to the obtained lower current values.

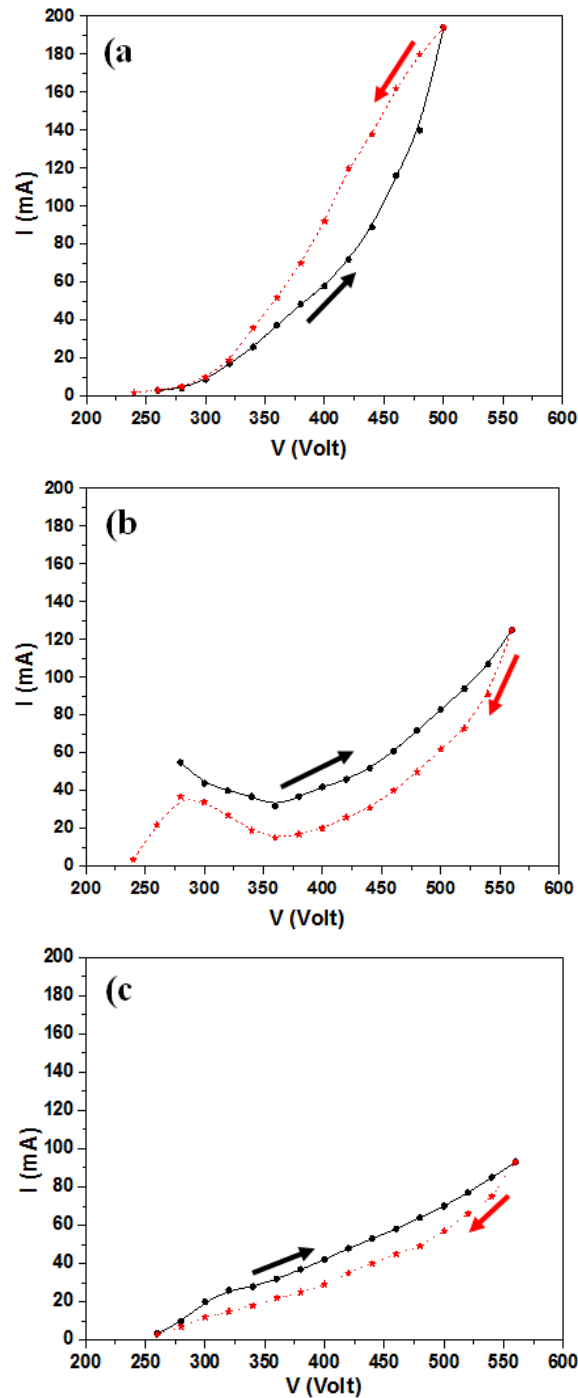


Fig. 1: Effect of target material on I-V characteristics at Ar^+ gas pressure of 0.05 mbar: (a) Cu; (b) Ni; (c) Cu-10wt.%Ni. (time period of each hysteresis loop is 2 min.)

It is also interesting to study the effect of both time period of hysteresis loop and gas type on the I-V characteristics of sputtering Cu, Ni and Cu-Ni targets separately at constant gas pressure (0.05 mbar) as shown in Figure 2(a-f). The following observations may be drawn:

- 1) Figure 2(a-c) clearly shows that the areas of the hysteresis loops (time taken for each hysteresis loop is approximately 20 min) are smaller than those obtained during a time period of approximately 2 min (Figure 1(a-c)). This means that the area of the hysteresis loop is related to its time period, it is larger at the lower time period and vice versa. We assume that the residual ionization formed during the first path of each cycle would be short lived and consequently less current values were obtained and small areas of the hysteresis loops were resulted.

- 2) As a result of sputtering Cu, Ni and Cu-Ni targets in a gas mixture of 75%Ar+25%O₂ at the same previous conditions of pressure and time, the obtained I-V characteristics showed hysteresis loops associated with higher current values (Figure 2(d-f)) than those obtained in dry Ar atmosphere (Figure 2(a-c)). The high current values can be attributed to the formation of different oxides on the target surface which enhanced the emission of secondary electrons and therefore the total current value was increased [19].
- 3) Hysteresis loops of Figure 2(d-f) also showed that all the sputtered targets have different transition zones at different voltages. The presence of these transition zones is attributed to the different types of oxides formed on the target surface as well as their different cohesive forces with the target.
- 4) For the Cu target (Figure 2d), as the applied voltage is decreased gradually, the corresponding current values depart to lower values from those previously obtained in the first path of the cycle, this is opposite to that obtained in Figure 2a. It is believed that the lower hysteresis leg obtained in this case is due to the formation of copper oxide layer which redeposited on the target surface (during the first path of the cycle) which consumed most of the ion energy as well as the deionization process of the gas ions caused by the excess number of emitted electrons from the formed oxides.

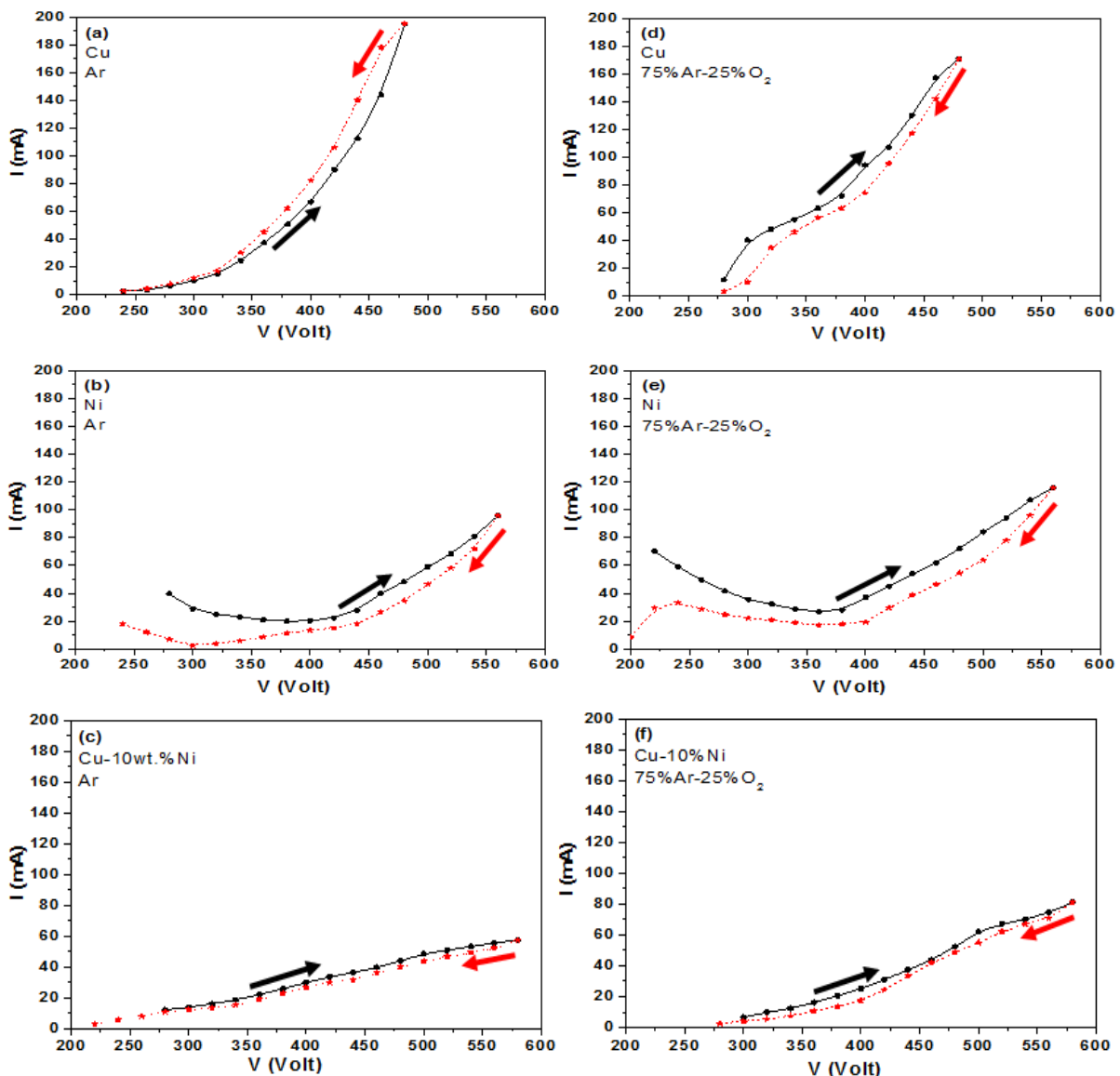


Fig. 2: Effect of gas type on plasma characteristics of sputtering different targets at gas pressure of 0.05 mbar. (time period of each hysteresis loop is 20 min.)

IV. Surface Topography:

Sputtering is usually accompanied by progressive morphological and compositional changes in the target surface. This is due to the fact that preferential sputtering of one of the target components leads to the formation of an alternated layer whose composition is different from the bulk.

Surface morphological features of sputtering Cu, Ni and Cu-Ni samples separately in dry atmospheres of Ar (Figure 3(a-c)) and 75% Ar+25% O₂ (Figure 3(d-f)) for 0.5 h are shown.

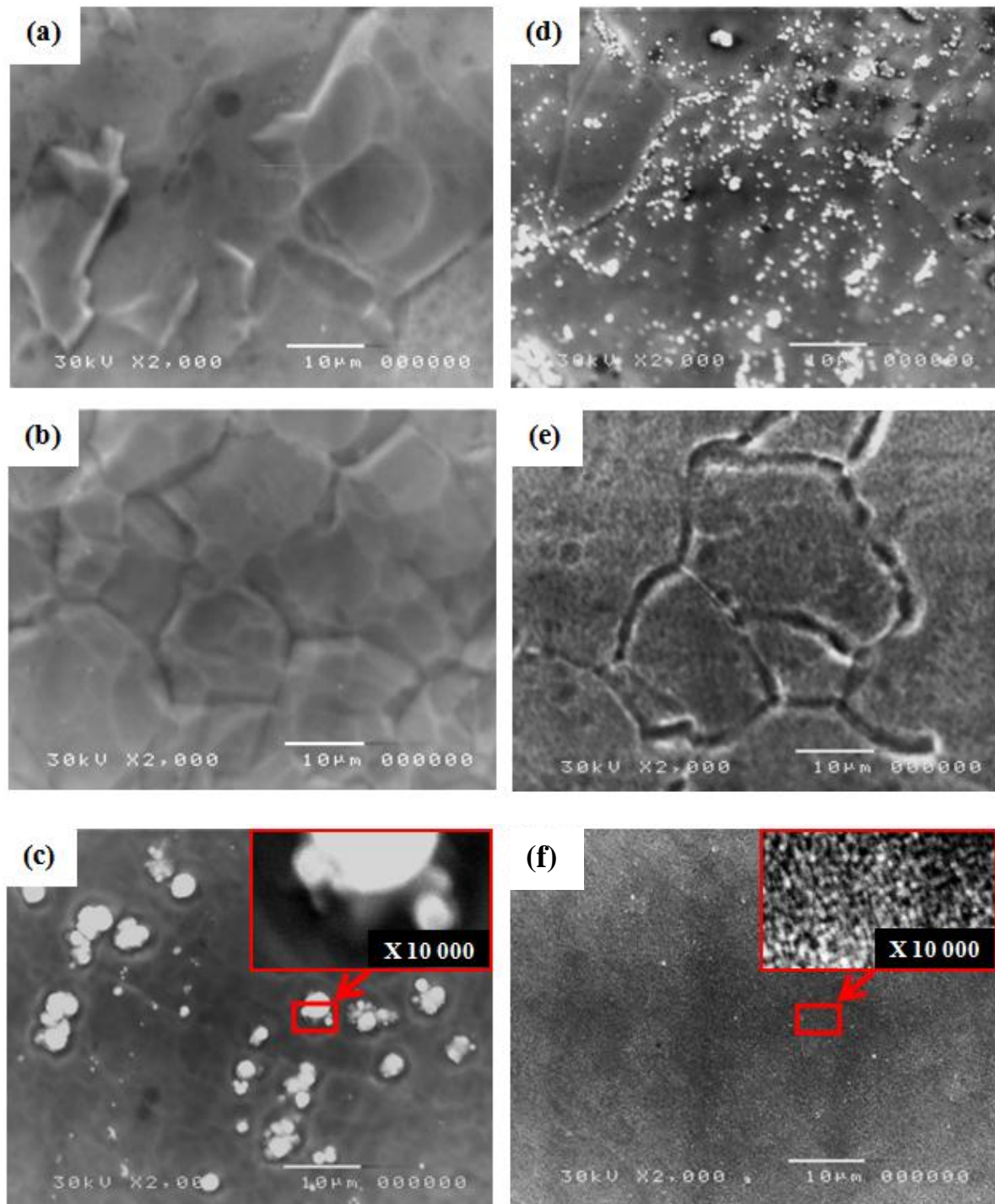


Fig. 3: Surface morphology of different samples developed in dc glow discharge at gas pressure 0.1 mbar for 0.5 h:

(a) Cu; (b) Ni; (c) Cu-10wt.%Ni (in dry Ar atmosphere).

(d) Cu; (e) Ni; (f) Cu-10wt.%Ni (in dry 75% Ar+25% O₂ atmosphere).

(X2 000).

From the first insight, one can realize that the surfaces of both Cu and Ni samples appeared almost eroded and free from any isolated particles with the appearance of some grains on the Ni surface (Figure 3(a & b)). On the other hand, the surface of Cu-Ni sample showed the formation of some scattered spherical protrusions with different sizes surrounded by etch pits as well as the appearance of some particle-depleted regions (Figure 3c). These protrusions were Cu_{3.8}Ni phase as mentioned earlier [14]. The morphological features of Figure 3c can be attributed to the presence of particles with different sputtering yields. Some particles (of high sputtering yield) are sputtered off the surface caused partial depletion of the surface from these particles, while other particles (of low sputtering yield) are remained on the surface leading to the formation of the observed protrusions.

On the other hand, surface morphological features of sputtered Cu, Ni and Cu-Ni samples in dry Ar/O₂ atmosphere (Figure 3(d-f)) were quite different from those observed in dry Ar atmosphere (Figure 3(a-c)). This is again due to the fact that adding oxygen gas to Ar glow discharge increased the current values causing more surface erosion and accordingly different surface morphological features were obtained.

It is interesting to compare surface morphological features of sputtered Cu, Ni and Cu-Ni samples in dry 75%Ar+25%O₂ atmosphere (Figure 3(d-f)) with those sputtered in dry Ar atmosphere (Figure 3(a-c)). The obtained results showed that:

- (i) Surface of sputtered Cu sample of Figure 3d appeared to be more eroded than that observed in Figure 3a with the formation of many scattered particles of different sizes.
- (ii) Surface of sputtered Ni sample of Figure 3e appeared to be more eroded than that observed in Figure 3b with the appearance of deeply eroded grain boundaries.
- (iii) Surface of sputtered Cu-Ni sample of Figure 3f appeared to be more rough than that observed in Figure 3c with the appearance of many tiny particles covering the whole surface as clearly observed in the inserted magnified figure.

V. Target Profile:

Sputtered atoms and molecules in their passage through the plasma region suffer many collisions with the sputtering gas ions and other sputtered species until they cool down to gas temperature and become thermalized ($kT \approx 0.025$ eV) at a certain distance (s) from the target's surface. At the edge of this distance, some atoms transport to the substrate by diffusion and others return back and deposit on the dead zone area of the target.

The formation of the backscattered material was previously reported by some authors [20-22] and was attributed to the presence of a virtual source in the distance between the cathode and substrate. For elemental targets there is only one virtual source is formed during sputtering in the magnetron sputtering system, while (n) virtual sources would be formed during sputtering of the compound targets. These virtual sources are formed at different distances s_i ($i=1, 2, \dots, n$) from the surface of the target where (n) is the number of elements in the target used.

Sputtering the three targets used in this work separately in inert and active gas atmospheres for constant sputtering time (0.5 h) at two different gas pressures namely; P_1 (0.05 mbar) and P_2 (0.1mbar) produced different rough circular deposits surrounded by smooth and continuous films in the dead zone areas of each target. These deposits were of different diameters and colours depending generally on target constituents, gas type, gas pressure as well as sputtering time.

In this work, we studied the influence of the above mentioned parameters on the formation of these deposits as shown in Figures (4&5) where the formed deposits diameters (D) were measured from these figures and given in Table (1), from which one can conclude the following remarks:

- (i) The deposit diameter of the Cu target is always larger than that obtained for the Ni target, when sputtered separately under the same conditions. This can be attributed to the fact that Cu has higher sputtering yield than that of Ni [16].
- (ii) The deposit diameter of the Cu-Ni target is larger than those obtained of both Cu and Ni targets for all conditions of gas type and gas pressure. This is due to the fact that there is only one virtual source was formed during sputtering of the elemental targets (Cu or Ni), while two virtual sources would be formed at different distances during sputtering of the Cu-Ni target which increased the redeposited material on the target surface.
- (iii) Adding oxygen gas (25%) to Ar glow discharge resulted in higher deposit diameters of the three targets than those obtained in Ar glow discharge. This can be attributed to the formation of different oxides on the target surface which enhanced both electron emission and sputtering rate and therefor more deposits with larger diameters were formed on the target.
- (iv) As the gas pressure increased from 0.05 mbar to 0.1 mbar the deposit diameter of each target was increased. This is believed due to the fact that as the gas pressure increased, more collisions occurred between plasma species and sputtered atoms and the distance of the virtual source from the target's surface decreased

causing an increase in the diameter of the formed deposit. This is in agreement with that previously postulated by Nyaiesh [21].

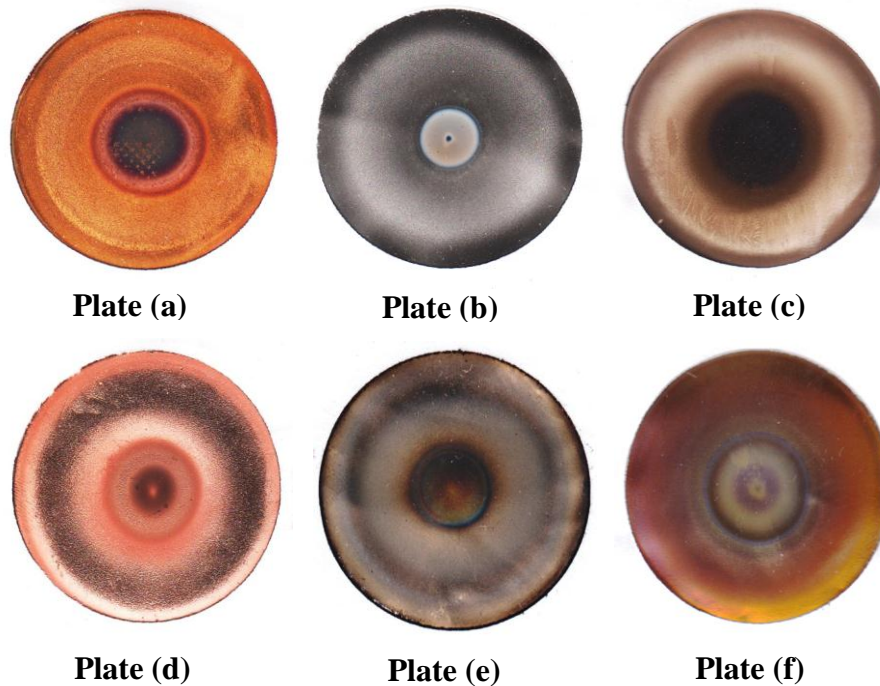


Fig. 4: Effects of gas type and target type on deposit diameter and colour due to sputtering the different targets at constant gas pressure of 0.05 mbar for 0.5 h:

- (a) Cu; (b) Ni; (c) Cu-10wt.%Ni (in dry Ar atmosphere).
(d) Cu; (e) Ni; (f) Cu-10wt.%Ni (in dry 75%Ar+25%O₂ atmosphere).

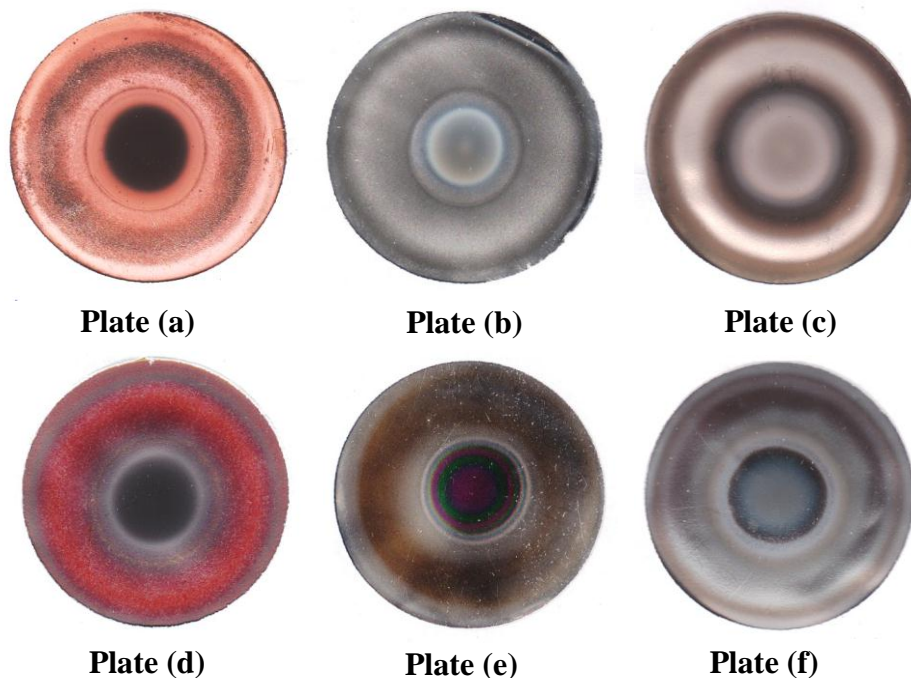


Fig. 5: Effects of gas type and target type on deposit diameter and colour due to sputtering the different targets at constant gas pressure of 0.1 mbar for 0.5 h:

- (a) Cu; (b) Ni; (c) Cu-10wt.%Ni (in dry Ar atmosphere).
(d) Cu; (e) Ni; (f) Cu-10wt.%Ni (in dry 75%Ar+25%O₂ atmosphere).

Table 1: Deposit diameter (D) for the targets used (sputtering time = 0.5 h)

Figure No.	Target	Gas Type	Gas Pressure (mbar)	Deposit Diameter D (mm)
Figure4. plate (a)	Cu	Ar	0.05	13
Figure4. plate (b)	Ni	Ar	0.05	11
Figure4. plate (c)	Cu/Ni	Ar	0.05	16
Figure4. plate (d)	Cu	75%Ar+25%O ₂	0.05	15.5
Figure4. plate (e)	Ni	75%Ar+25%O ₂	0.05	14
Figure4. plate (f)	Cu/Ni	75%Ar+25%O ₂	0.05	17.5
Figure5. plate (a)	Cu	Ar	0.1	15
Figure5. plate (b)	Ni	Ar	0.1	13
Figure5. plate (c)	Cu/Ni	Ar	0.1	20
Figure5. plate (d)	Cu	75%Ar+25%O ₂	0.1	17.5
Figure5. plate (e)	Ni	75%Ar+25%O ₂	0.1	16
Figure5. plate (f)	Cu/Ni	75%Ar+25%O ₂	0.1	23

VI. Conclusions:

Different topics dealing with sputtering of Cu, Ni and Cu-10wt.%Ni targets in inert and active gas atmospheres using a dc planar magnetron sputtering system were conducted. The main conclusions were drawn as follows:

- I-V characteristics of Cu, Ni and Cu-Ni targets in dry atmospheres of Ar and Ar/O₂ showed that the Cu target gave greater current values at all values of applied voltages as compared with those of both Ni and Cu-Ni targets.
- I-V characteristics of the three targets in a gas mixture of Ar/O₂ at the same conditions of pressure and time showed hysteresis loops associated with higher current values than those obtained in dry Ar atmosphere.
- The area of the hysteresis loop (of each target) is related to the time period of the loop, it is larger at the lower time period and vice versa.
- Surface morphological features of sputtered Cu, Ni and Cu-Ni samples in dry Ar/O₂ atmosphere appeared to be more eroded than those observed in dry Ar atmosphere.
- The deposit diameter of the Cu/Ni target was larger than those obtained of both Cu and Ni targets, when sputtered separately under the same conditions.
- Adding oxygen gas (25%) to Ar glow discharge resulted in higher deposit diameters of the three targets than those obtained in Ar glow discharge.
- As the gas pressure was increased, the deposit diameter of each target was also increased.

References

- [1]. Ohring, M., 2002. "Materials science of thin films," 2nd edition, academic press, San Diego, New York, Boston, London.
- [2]. Kucharska, B. and E. Kulej, 2010. X-ray measurement of the Cu/Ni multilayer period. Archives of metallurgy and materials, 55, 1: 45-51.
- [3]. Zhu, H.L., J. Y. Zhang, C. Z. Li, F. Pan, T. M. Wang, and B. B. Huang, 2009. Cu₂O thin films deposited by reactive direct current magnetron sputtering. Thin solid films, 517(19): 5700–5704.
- [4]. Tvarozek, V., K. Shtereva, I. Novotny, J. Kovac, P. Sutta, R. Smanek and A. Vincze, 2008. RF diode reactive sputtering of n-and p-type zinc oxide thin films. Vacuum, 82: 166-169.
- [5]. Reddy, A.S., S. Uthanna and P.S. Reddy, 2007. Properties of dc magnetron sputtered Cu₂O films prepared at different sputtering pressures. Appl. Surf. Sci., 253(12): 5287–5292.
- [6]. Jo, Y.D., K.N. Hui, K.S. Hui, Y.R. Cho and K.H. Kim, 2014. Microstructural, optical, and electrical properties of Ni–Al co-doped ZnO films prepared by dc magnetron sputtering. Materials research bulletin, 51: 345–350.
- [7]. Cen, J. and D. Wang, 2012. The metallization of PTC ceramic by magnetron sputtering. Physics procedia, 32: 482–486.
- [8]. Mech, K., R. Kowalik and P. Zabinski, 2011. Cu thin films deposited by dc magnetron sputtering for contact surfaces on electronic components. Archives of metallurgy and materials, 56, 4: 903-908.
- [9]. Kim, Nam-Hoon, Dong-Myong Na, Pil-Ju Ko, Jin-Seong Park and Woo-Sun Lee, 2007. Electrical and thermal properties of platinum thin films prepared by dc magnetron sputtering for micro-heater of microsensor applications after CMP process. Solid state phenomena vols., 124-126: 267-270
- [10]. Mugwang, F.K., P.K. Karimi, W.K. Njoroge, O. Omayio and S.M. Waita, 2013. Optical characterization of copper oxide thin films prepared by reactive dc magnetron sputtering for solar cell applications. Int. J. Thin Film Sci. Tec., 2 No. 1: 15-24.
- [11]. Chernysh, V.S. and A.S. Patraakeev, 2012. Angular distribution of atoms sputtered from alloys. Nuclear instruments and methods in physics research B, 270: 50–54.
- [12]. Wu, Chia-Che and Fan-Bean Wu, 2009. Microstructure and mechanical properties of magnetron co-sputtered Ni–Al coatings. Surface & coatings technology, 204: 854–859.

- [13]. Shulga, V.I., 2008. An attempt to solve andersen's puzzle in surface segregation during alloy sputtering. Nuclear instruments and methods in physics research B, 266: 5107–5111.
- [14]. Soliman, H.N., H.M. Hosni and A. Rizk, 2014. Effects of physical sputtering and annealing temperature on surface behaviour of Cu-10wt.%Ni alloy, Accepted for publication in Egypt. J. Solids.
- [15]. Soliman, H.N. and A. Rizk, 2015. Effects of annealing temperatures on surface microtexturing and composition of Cu-10wt.%Ni-2wt.%Sn alloy due to Ar⁺ bombardment in a magnetron sputtering system. Current science international, 4: 216-224 .
- [16]. Carter, G. and J.S. Colligon, 1968. Ion bombardment of solids, New York, American Elsevier Pub. Co.
- [17]. Lam, N.Q. and K. Johannessen, 1992. Physical sputtering of Cu-Ni alloys: a molecular dynamics study. Nuclear instruments and methods in physics research B, 71: 371-380.
- [18]. Kudriavtsev, Y., A. Villegas, A. Godines and R. Asomoza, 2005. Calculation of the surface binding energy for ion sputtered particles. Applied surface science, 239: 273–278.
- [19]. Maniv, S. and W.D. Westwood, 1980. Discharge characteristics for magnetron sputtering of Al in Ar and Ar/O₂ mixtures. J. Vac. Sci.Technol., 17(3): 743.
- [20]. Rizk, N.S., A. Rizk and S.K. Habib, 1990. Redeposition of backscattered material in a dc magnetron sputtering system. Vacuum., 40(3): 245-249.
- [21]. Nyaiesh, A.R., 1986. Target profile change during magnetron sputtering. Vacuum, 36(6): 307-309.
- [22]. Nyaiesh, A.R. and L. Holland, 1982. Reactive magnetron sputtering of titanium and its oxides, J. Vac. Sci., Technol., 20: 1389.